

# Folding Pathway of FKBP12 and Characterisation of the Transition State

Ewan R. G. Main, Kate F. Fulton and Sophie E. Jackson\*

Cambridge University Chemical  
Laboratory, Lensfield Road  
Cambridge, CB2 1EW, UK

The folding pathway of human FKBP12, a 12 kDa FK506-binding protein (immunophilin), has been characterised. Unfolding and refolding rate constants have been determined over a wide range of denaturant concentrations and data are shown to fit to a two-state model of folding in which only the denatured and native states are significantly populated, even in the absence of denaturant. This simple model for folding, in which no intermediate states are significantly populated, is further supported from stopped-flow circular dichroism experiments in which no fast “burst” phases are observed. FKBP12, with 107 residues, is the largest protein to date which folds with simple two-state kinetics in water ( $k_F = 4 \text{ s}^{-1}$  at 25 °C). The topological crossing of two loops in FKBP12, a structural element suggested to cause kinetic traps during folding, seems to have little effect on the folding pathway.

The transition state for folding has been characterised by a series of experiments on wild-type FKBP12. Information on the thermodynamic nature of, the solvent accessibility of, and secondary structure in, the transition state was obtained from experiments measuring the unfolding and refolding rate constants as a function of temperature, denaturant concentration and trifluoroethanol concentration. In addition, unfolding and refolding studies in the presence of ligand provided information on the structure of the ligand-binding pocket in the transition state. The data suggest a compact transition state relative to the unfolded state with some 70% of the surface area buried. The ligand-binding site, which is formed mainly by two loops, is largely unstructured in the transition state. The trifluoroethanol experiments suggest that the  $\alpha$ -helix may be formed in the transition state. These results are compared with results from protein engineering studies and molecular dynamics simulations (see the accompanying paper).

© 1999 Academic Press

*Keywords:* immunophilin; FKBP12; protein folding; transition state; two-state folding

\*Corresponding author

## Introduction

Since 1968, when Levinthal first proposed that proteins could not fold by a random search of conformational space (Levinthal, 1968), it has been widely accepted that proteins must have defined folding pathways. Many experimental studies have attempted to characterise folding pathways.

Abbreviations used: FKBP12, FK506 binding protein; GdnHCl, guanidinium chloride; TFE, trifluoroethanol; CD, circular dichroism; UV, ultraviolet; PBS, phosphate-buffered saline; PPIase, peptidyl-prolyl isomerase; GST, glutathione *S*-transferase.

E-mail address of the corresponding author:  
sej13@cam.ac.uk

Initially, the protein folding field was dominated by the study of proteins which folded through stable intermediate states which were populated and could thus be characterised (Evans & Radford, 1994). In 1991, however, it was shown that stable intermediates were not essential for the fast efficient folding of a protein (Jackson & Fersht, 1991a) and it has subsequently been suggested that stable intermediates may slow the folding process (Fersht, 1995). More than 20 small proteins have now been shown to fold with simple two-state kinetics (Jackson, 1998), and it is likely that many other small proteins, or domains of larger proteins, will also fold in this way. Here we present studies on human FK506-binding protein, FKBP12, and

show that, despite its size and structure, it too folds according to a two-state model.

Human FKBP12 is a 12 kDa protein, 107 residues in length. It is the major cytosolic immunophilin (immunosuppressant-binding protein) in mammalian cells and inhibits T-cell proliferation when bound to FK506 or rapamycin (Kay, 1996). It contains no disulphide bridges, and all of its seven proline residues are in a *trans* conformation in the native state, thus the folding will not be limited by disulphide bond formation or rearrangement, or proline isomerisation. In addition, it has been shown that FKBP12 undergoes a reversible two-state unfolding under equilibrium conditions which can be induced using urea or guanidinium chloride (GdnHCl) (Egan *et al.*, 1993). The urea and GdnHCl-induced denatured states have been characterised using NMR spectroscopy which has shown that, although there is some evidence for fleeting residual structure, there is no evidence for extensive structure in the unfolded state (Logan *et al.*, 1994). The structure of native FKBP12, which has been solved by X-ray crystallography and NMR spectroscopy (Michnick *et al.*, 1991; van Duynes *et al.*, 1991), is outlined below and shows some interesting features which may affect the folding pathway.

The structure of FKBP12 is characterised by a large, amphiphilic, antiparallel five-stranded  $\beta$ -sheet with +3, +1, -3, -1 topology (see Figure 1). An amphiphilic  $\alpha$ -helix packs against the hydrophobic face of the  $\beta$ -sheet at an angle of  $60^\circ$  with respect to the long axis. The  $\beta$ -sheet has a right-handed twist and wraps around the helix to form a well-ordered hydrophobic core. The immunosuppressant-binding site, which contains many aromatic side-chains, forms a large, shallow hydrophobic pocket between the  $\alpha$ -helix and  $\beta$ -sheet. A notable feature of FKBP12 resulting from the +3, +1, -3, -1 topology of the  $\beta$ -sheet is a topological crossing of loop-1 (Pro9-Gln20 which connects  $\beta$ -strand 1 and  $\beta$ -strand 2), and loop-4 (Ala64-Gln70 which connects the  $\alpha$ -helix to  $\beta$ -strand 4). Although crossing topologies have been observed in proteins containing parallel  $\beta$ -sheets, they are rare in antiparallel  $\beta$ -sheet structures (Michnick *et al.*, 1991). It has been suggested that the topological crossing of loops may result in complex folding pathways which would slow folding, and may even result in misfolded species which would form kinetic traps on the folding pathway (Michnick *et al.*, 1991).

A number of different experimental approaches have been used to study the structure and energetics of folding transition states. Two main strategies have been adopted; the first is to study wild-type protein and measure the rates of unfolding and refolding as experimental conditions such as temperature, denaturant concentration, ligand concentration, etc. are varied. This provides low-resolution information on the thermodynamic nature of the transition state, as well as its compactness, as measured by burial of hydrophobic side-chains.

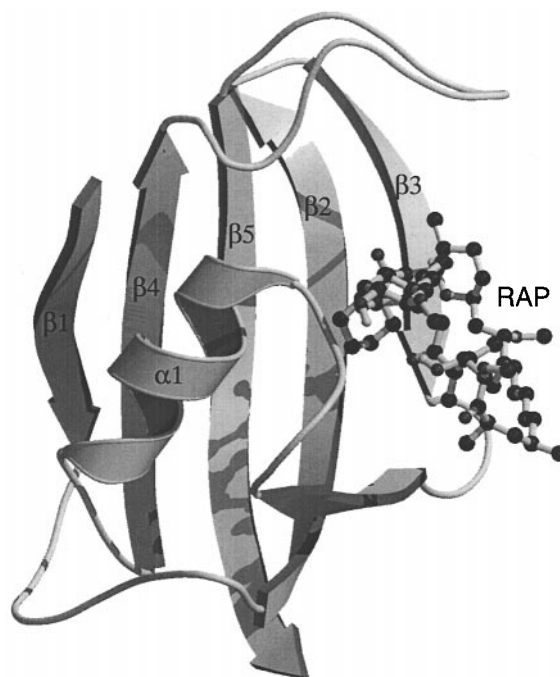


**Figure 1.** Structure of the human FKBP12-rapamycin complex. The major secondary structural features of FKBP12 are a large, amphiphilic, five-stranded antiparallel  $\beta$ -sheet with a +3, +1, -3, -1 topology and a small, amphiphilic  $\alpha$ -helix. The  $\alpha$ -helix, from Ile56 to Val63, packs against the hydrophobic face of the  $\beta$ -sheet to form the main hydrophobic core of the protein. The  $\beta$ -sheet comprises of  $\beta$ -strand 1 (Val2 to Ser8),  $\beta$ -strand 4 (Arg71 to Ile76),  $\beta$ -strand 5 (Leu97 to Leu106),  $\beta$ -strand 2 (Thr21 to Leu30),  $\beta$ -strand 3, which splits into two (Lys35 to Ser38 and Phe46 to Met49). The rapamycin-binding site comprises residues Tyr26, Phe46, Val55, Ile56, Trp59 and Phe99. Rapamycin (RAP) is shown using a ball-and-stick representation. The secondary structure representation was produced using MOLSCRIPT (Kraulis, 1991) and rendered using Raster3D (Merritt & Murphy, 1994).

Studies on the folding and unfolding of wild-type proteins in the presence and absence of ligand have yielded information on structure formation in ligand-binding pockets during folding (Sancho *et al.*, 1991). Recently, this type of approach has been extended by studying the effect of sugars and alcohols on the rate of folding and unfolding (Chiti *et al.*, 1998, 1999). These experiments have yielded information on the extents of hydration and secondary structure, particularly  $\alpha$ -helices, in the transition state. The second approach is to use protein engineering techniques, and measure the relative stabilities and rates of folding of wild-type and mutant protein. The  $\Phi$ -value analysis is then used to quantitatively measure the energetics of structure formation in the transition state (Fersht *et al.*, 1992). This experimental approach, which provides detailed, residue-specific information on the energetics of the transition state for folding, has been complemented by molecular dynamic simulations

which have provided structural information on the transition state (Daggett *et al.*, 1996, 1998; Li & Daggett, 1996; Ladurner *et al.*, 1998).

Here and in the accompanying paper (Fulton *et al.*, 1999), we present a comprehensive characterisation of the pathway of folding and transition state for folding of FKBP12. We have employed both experimental approaches outlined above, as well as performing molecular dynamic simulations, to give a highly detailed picture of both the energetics and structure of the transition state for folding. The results obtained using the two different experimental techniques are compared, as are the results obtained from theoretical simulations and experiment. This is the first example of the use of all three approaches to characterise the transition state for folding of a single protein.

## Results

### Equilibrium experiments

Figure 2(a) and (b) show the change in the fraction of unfolded FKBP12 upon titration with chemical denaturants urea or guanidinium chloride (GdnHCl). There is a single, sharp transition between the initial and final states indicating that FKBP12 unfolds cooperatively according to a two-state model under equilibrium conditions, as has been shown previously (Egan *et al.*, 1993). The fluorescence-monitored unfolding has been shown to correspond to a global denaturation of the protein (Egan *et al.*, 1993). The entire data set can be fitted directly to equation (8) (see Materials and Methods), from which the value of  $[D]_{50\%}$ , the midpoint of unfolding and  $m_{U-F}$ , a constant that is proportional to the increase in degree of exposure of the protein on unfolding, can be calculated (Table 1). The values of  $\Delta G_{U-F}^{H_2O}$  obtained from either urea ( $5.53(\pm 0.12)$  kcal mol<sup>-1</sup>) or GdnHCl ( $5.13(\pm 0.21)$  kcal mol<sup>-1</sup>) denaturation using equation (9) (see Materials and Methods) are very similar, and fall within the range of values obtained for other globular proteins (Robertson & Murphy, 1997).

Figure 2(a) also illustrates the effect of small concentrations of trifluoroethanol (TFE) on the stability of the native state of the protein as measured by urea-induced denaturation curves. Low concentrations of TFE (3.6–9.6% (v/v)) stabilise the native state of FKBP12 relative to the unfolded state by up to 1.1 kcal mol<sup>-1</sup>, whereas higher concentrations (17% (v/v)) destabilise the protein by some 0.4 kcal mol<sup>-1</sup> (Table 1). TFE is known to weaken hydrophobic interactions (Lu *et al.*, 1997) and to stabilise secondary structure (Nelson & Kallenbach, 1989; CammersGoodwin *et al.*, 1996; Walgers *et al.*, 1998), and high concentrations of TFE are known to unfold proteins by stabilising non-native  $\alpha$ -helices in the unfolded state (Narhi *et al.*, 1996; Sivaraman *et al.*, 1996). The TFE unfolding of FKBP12 is shown in Figure 2(c).

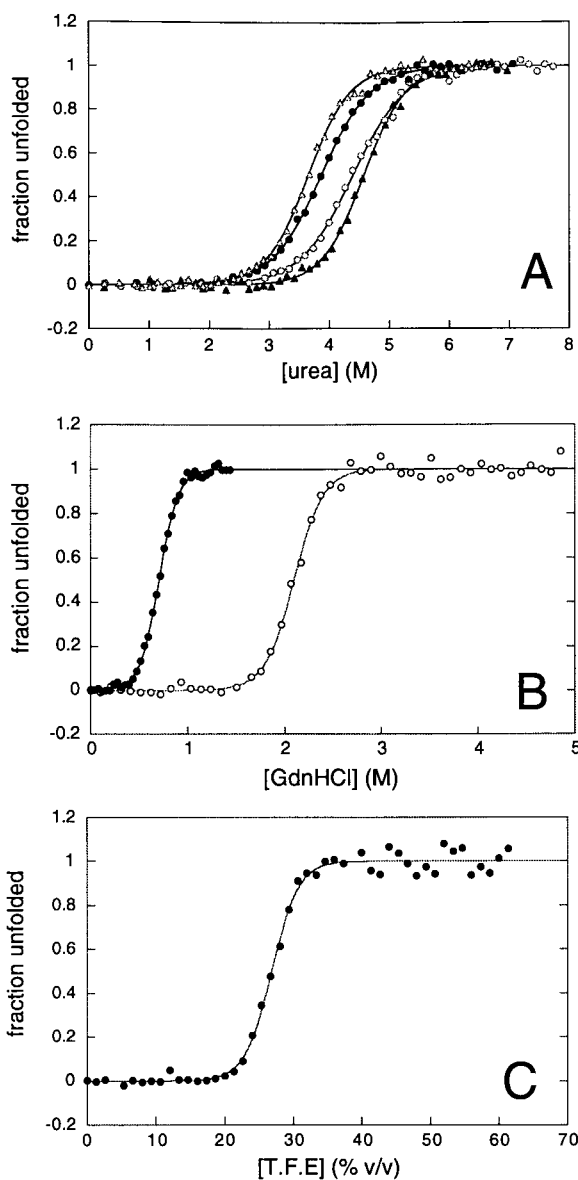


**Figure 2.** Equilibrium unfolding experiments. (a) Urea-induced unfolding of wild-type FKBP12 in 0% TFE (filled circles), 3.64% TFE (open circles), 9.6% TFE (filled triangles) and 17% TFE (open triangles). (b) Guanidinium chloride-induced unfolding of wild-type FKBP12 in the absence (filled circles) and presence of 20  $\mu$ M rapamycin (open circles). (c) Trifluoroethanol (TFE)-induced unfolding of wild-type FKBP12. Unfolding was monitored using fluorescence spectroscopy and data has been normalised for comparative purposes. All experiments were performed at 25  $^{\circ}$ C, in 50 mM Tris-HCl (pH 7.5), 1 mM DTT. The continuous curves show the best fit of the data to equation (8). The thermodynamic parameters calculated from these fits are shown in Table 1.

Figure 2(b) shows the normalised unfolding curve for the GdnHCl-induced denaturation of free and complexed FKBP12. In both cases data can be fitted to a two-state model of unfolding

**Table 1.** Thermodynamic parameters for the equilibrium unfolding of wild-type FKBP12 by different denaturants

Experiment <sup>a</sup>	Denaturant	$m_{U-F}^b$ (kcal mol <sup>-1</sup> M <sup>-1</sup> )	$[D]_{50\%}^b$ (M)	$\Delta G_{U-F}^{H_2O^c}$ (kcal mol <sup>-1</sup> )	$\Delta G_{U-F}^{H_2O^g}$ (kcal mol <sup>-1</sup> )	$\Delta\Delta G_{U-F}^{H_2O^f}$ (kcal mol <sup>-1</sup> )
FKBP12	Urea	1.43 ± 0.03	3.87 ± 0.01	5.53 ± 0.12	6.15 ± 0.08	
FKBP12 + 3.6% TFE	Urea	1.34 ± 0.07	4.40 ± 0.03	5.90 ± 0.31	7.00 ± 0.10	0.84 ± 0.05
FKBP12 + 9.6% TFE	Urea	1.70 ± 0.09	4.58 ± 0.03	7.79 ± 0.42	7.28 ± 0.10	1.13 ± 0.05
FKBP12 + 17% TFE	Urea	1.68 ± 0.04	3.65 ± 0.01	6.13 ± 0.15	5.80 ± 0.07	-0.35 ± 0.02
FKBP12	GdnHCl	6.60 ± 0.27	0.778 ± 0.005	5.13 ± 0.21		
FKBP12 + rapamycin	GdnHCl	3.91 ± 0.27	2.10 ± 0.01	8.21 ± 0.57		
FKBP12	TFE	0.30 ± 0.03 <sup>d</sup>	26.8 ± 0.20 <sup>e</sup>	8.15 ± 0.81		

<sup>a</sup> Experimental conditions are 50 mM Tris-HCl, 1 mM DTT (pH 7.5), 25 °C unless otherwise stated.

<sup>b</sup> Calculated using equation (8).

<sup>c</sup> Calculated from  $\Delta G_{U-F}^{H_2O} = m_{U-F} [D]_{50\%}$ .

<sup>d</sup> Units are kcal mol<sup>-1</sup>%<sup>-1</sup>.

<sup>e</sup> Units are %.

<sup>f</sup> Calculated using the equation  $\Delta\Delta G_{U-F}^{H_2O} = \langle m \rangle \{ [D]_{50\%} - [D]_{50\%} \}$  where  $\langle m \rangle$  is the average  $m$ -value determined for multiple experiments on wild-type and mutant FKBP12 (1.59(±0.02); Main *et al.*, 1998),  $[D]_{50\%}$  is the midpoint of unfolding in 3.6, 9.6 or 17% TFE, and  $[D]_{50\%}$  is the value in 0% TFE.

<sup>g</sup> Calculated from  $\Delta G_{U-F}^{H_2O} = m_{U-F} [D]_{50\%}$  using an average  $m_{U-F}$  value of 1.59(±0.02).

(equation (8)). The presence of 20 μM rapamycin, which is a tight-binding ligand ( $K_d = 0.2$  nM) (Bierer *et al.*, 1990), stabilises the folded state relative to the unfolded state. An apparent difference in free energy of unfolding between free and complexed FKBP12,  $\Delta G_{app}$ , can be calculated, and, if the ligand concentration is known, used to calculate  $K_d$  using equation (1) (Meiering, 1992):

$$\Delta G_{app} = \Delta G_{U-F}^{H_2O} + RT \ln(1 + [L]/K_d) \quad (1)$$

where  $[L]$  is the ligand concentration, and  $K_d$  the dissociation constant for the protein-ligand complex. For FKBP12 it is difficult to calculate  $\Delta G_{app}$  accurately because of the difference in  $m_{U-F}$  between free and complexed FKBP12. Although the difference is much larger than normally observed for wild-type and mutant proteins (Jackson *et al.*, 1993) it can be attributed to the non-linearity of  $\Delta G_{U-F}$  with respect to  $[D]$  at low concentrations of GdnHCl. Estimates of  $m_{U-F}$  can be obtained at different  $[GdnHCl]$  using Tanford's model relating  $m_{U-F}$  to  $\alpha$ , the fractional degree of exposure of residues on unfolding, and the amino acid composition of the protein (Tanford, 1968, 1970), and following the analysis of Ahmad & Bigelow (1986). For FKBP12,  $m_{U-F}$  is proportional to  $7.8[GdnHCl]^{-0.4}$ , which predicts an increase in  $m_{U-F}$  by a factor of 1.5 between 0.8 M and 2.1 M GdnHCl, the midpoints of unfolding of free and complexed FKBP12, respectively. This prediction is in agreement with the experimentally determined values taking into account experimental error. Thus, the low value for  $m_{U-F}$  for the FKBP12-rapamycin complex reflects intrinsic changes in  $m_{U-F}$  with  $[GdnHCl]$ .

### Unfolding kinetics

The unfolding of FKBP12 is monophasic, and data can be fitted to a single exponential. The observed first-order rate constant is found to increase exponentially with increasing  $[D]$ , in

accordance with equation (2):

$$\ln k_U = \ln k_U^{H_2O} + m_{\ddagger-F} [D] \quad (2)$$

where  $k_U$  is the rate constant of unfolding at a given denaturant concentration,  $k_U^{H_2O}$  is the rate constant of unfolding in water,  $m_{\ddagger-F}$  is the slope, and  $[D]$  the final denaturant concentration. The plot of  $\ln k_U$  versus  $[D]$  for the urea unfolding of FKBP12 is linear over the concentration range used (Figure 3(a)). Values for  $k_U^{H_2O}$  and  $m_{\ddagger-F}$  are shown in Table 2. The plot of  $\ln k_U$  versus  $[D]$  for the GdnHCl-unfolding, however, shows slight deviations from linearity (Figure 3(b)). Such non-linearity has been observed for other proteins and may result from small movements in the position of the transition state with denaturant concentration (Matouschek & Fersht, 1993; Matouschek *et al.*, 1995). To account for this non-linearity the data were also fitted to a second-order polynomial equation:

$$\ln k_U = \ln k_U^{H_2O} + m_{\ddagger-F} [D] + m_{\ddagger-F}^* [D]^2 \quad (3)$$

where  $m_{\ddagger-F}$  and  $m_{\ddagger-F}^*$  are the coefficients for the first and second-order  $[D]$  terms, respectively. The slope of the plot at a particular GdnHCl concentration is given by  $m_{\ddagger-F}^{[D]} = m_{\ddagger-F} + 2m_{\ddagger-F}^* [D]$ . Values for  $\ln k_U^{H_2O}$ ,  $m_{\ddagger-F}$  and  $m_{\ddagger-F}^*$  calculated using equation (3) for the GdnHCl unfolding data are  $-8.78(\pm 0.17)$ ,  $5.46(\pm 0.17)$  M<sup>-1</sup>, and  $-0.47(\pm 0.04)$  M<sup>-2</sup>, respectively.

### Refolding kinetics

The refolding of FKBP12 is at least a triphasic process in 50 mM Tris-HCl (pH 7.5), 1 mM DTT at 25 °C. The multiphasic nature of the refolding reaction results from a heterogeneous population in the denatured state due to proline isomerisation. The fast folding phase, 67% of the amplitude measured by stopped-flow spectroscopy, corresponds to the folding of the fraction of protein that has all its

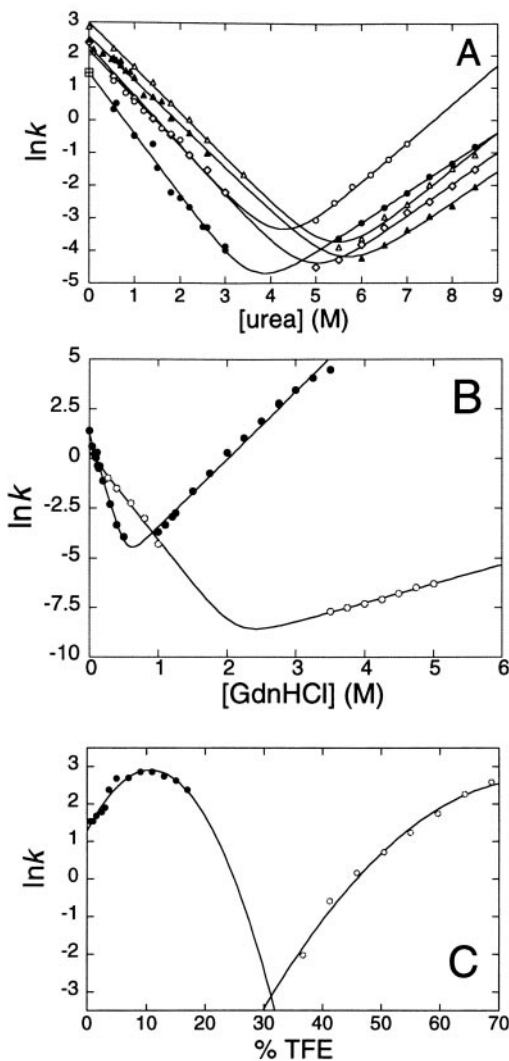


**Figure 3.** Kinetic unfolding and refolding experiments. (a) [Urea]-dependence of the natural logarithm of the rate constants for unfolding and refolding of FKBP12. Rate constants are measured at 25 °C, in 50 mM Tris-HCl (pH 7.5), 1 mM DTT. Points between 0.54 and 8 M were obtained by [urea]-jump experiments (filled circles), the point at 0 M urea was obtained by acid-jump, or alkali-jump experiment (hatched square). Each point is the average of at least five separate experiments. Also shown are the rates measured in 0.4 M Na<sub>2</sub>SO<sub>4</sub> (filled triangles), 3.6% TFE (open diamonds), 9.6% TFE (open triangles), and 17% TFE (open circles). The continuous curves show the best fit of the data to a two-state model (equation (5)). (b) [GdnHCl]-dependence of the natural logarithm of the refolding rate constant for FKBP12 (filled circles) and the complex formed between FKBP12 and rapamycin (open circles). Other experimental details are as in (a). The continuous curves show the best fit of the data to a two-state model (equation (5)). (c) [TFE]-dependence of the natural logarithm of the rate constants for unfolding and refolding of FKBP12. Rate constants are measured at 25 °C, in 50 mM Tris-HCl (pH 7.5), 1 mM DTT. Points between 0 and 3% TFE were obtained by pH-jump experiment (filled circles), between 3.6 and 20% TFE by [TFE]-jump refolding experiment (filled circles), and between 36 and 60% TFE by [TFE]-jump unfolding experiment (open circles). The continuous curve shows the best fit of the unfolding and refolding data to a second-order polynomial.

proline residues in a *trans* conformation in the denatured state. The following discussion applies only to the fast phase; characterisation of the slower phases and evidence that these correspond to rate-limiting proline isomerisation reactions is discussed below.

The [denaturant]-jump experiments were used to measure the rate constant for folding between 0.54 and 3.0 M for urea, and 0.1–0.5 M for GdnHCl. The rate is found to decrease exponentially with increasing [D], in accordance with equation (4), Figure 3(a) and (b). In addition, pH-jump experiments were employed to measure the rate of folding in the absence of denaturant. The rate of folding measured by acid-jump ( $k_F = 4.1 \text{ s}^{-1}$ ) or alkali-jump ( $k_F = 4.0 \text{ s}^{-1}$ ) experiments are within experimental error of the extrapolated rate calculated from the [denaturant]-jump experiments.

If folding is a reversible transition between just two states, the native and denatured state, then the rate constant for folding,  $k_F$ , must follow the rate law:

$$\ln k_F = \ln k_F^{\text{H}_2\text{O}} - m_{\ddagger-U}[D] \quad (4)$$

where  $k_F$  is the rate constant of refolding at a given denaturant concentration,  $k_F^{\text{H}_2\text{O}}$  is the rate constant of refolding in water, and  $m_{\ddagger-U}$  is the slope. The complete kinetics of folding and unfolding can be fitted to equation (5), which is derived from equations (2) and (4):

$$\ln k = \ln(k_F^{\text{H}_2\text{O}} \exp(-m_{\ddagger-U}[D]) + k_U^{\text{H}_2\text{O}} \exp(m_{\ddagger-F}[D])) \quad (5)$$

where  $k$  is the rate of unfolding or refolding at a particular denaturant concentration (Jackson & Fersht, 1991a). The kinetic data for urea or GdnHCl unfolding and refolding of FKBP12 can be fitted to this two-state model to yield the values for  $k_F^{\text{H}_2\text{O}}$ ,  $k_U^{\text{H}_2\text{O}}$ ,  $m_{\ddagger-U}$  and  $m_{\ddagger-F}$  (Table 2). The value for  $k_F^{\text{H}_2\text{O}}$  calculated from the best fit of the urea and GdnHCl data are within experimental error. When the GdnHCl data are fitted to equation (5),  $k_U^{\text{H}_2\text{O}}$  is slightly higher than that measured for the urea experiment; however, when curvature in the unfolding data is taken into consideration (equation (3)), the values of  $k_U^{\text{H}_2\text{O}}$  extrapolated from the urea and GdnHCl unfolding data are identical (Table 2).

From these results the values for  $\Delta G_{U-F}^{\text{H}_2\text{O}}$  and  $m_{U-F}$  can be calculated taking into account the equilibria in the denatured state due to proline isomerisation (Jackson & Fersht, 1991a). The values are summarised in Table 3. For the urea experiments the values obtained from the kinetic experiments are within experimental error of the values obtained directly from the equilibrium experiments. For the GdnHCl experiments the values do not agree quite as well, possibly as a result of curvature in the unfolding plots.

**Table 2.** Kinetic parameters from unfolding and refolding experiments

	$k_F^{H_2O}$ (s <sup>-1</sup> )	$m_{\ddagger-U}$ (M <sup>-1</sup> )	$k_U^{H_2O}$ ( $\times 10^{-5}$ s <sup>-1</sup> )	$m_{\ddagger-F}$ (M <sup>-1</sup> )	$\beta_{\ddagger}$ kin	$\beta_{\ddagger}^d$ eqm
<b>A. urea</b>						
FKBP12	4.3 ± 0.5	1.87 ± 0.06	17 ± 7	0.92 ± 0.06	0.7	0.6
+0.4 M Na <sub>2</sub> SO <sub>4</sub>	12.7 ± 0.7	1.32 ± 0.04	ND	ND		
<b>B. +TFE</b>						
+0% TFE	4.4 ± 0.5	1.86 ± 0.06	13 ± 5	0.97 ± 0.05	0.7	0.6
+3.6% TFE	9.6 ± 0.6	1.51 ± 0.03	5.7 ± 1.6	0.98 ± 0.04	0.6	0.6
+9.6% TFE	19.8 ± 1.3	1.37 ± 0.03	2.8 ± 1.1	1.12 ± 0.05	0.6	0.6
+17% TFE	8.4 ± 0.8	1.46 ± 0.07	11.4 ± 5.7	1.20 ± 0.08	0.6	0.5
<b>C. GdnHCl</b>						
FKBP12	3.4 ± 0.4 <sup>a</sup> 3.3 ± 0.2 <sup>b</sup>	11.6 ± 0.4 <sup>a</sup> 11.1 ± 0.3 <sup>b</sup>	110 ± 20 <sup>a</sup> 17 ± 5 <sup>b</sup>	3.4 ± 0.1 <sup>a</sup> 5.4 ± 0.3 <sup>b</sup> (-0.45 ± 0.07)	0.8	0.7
+rapamycin	1.4 ± 0.2	4.39 ± 0.21	1.5 ± 0.6	0.96 ± 0.09	0.8	0.85

<sup>a</sup> Calculated from the best fit of the data to equation (5).  
<sup>b</sup> Calculated from the best fit of the data to a two-state model using a second-order polynomial fit for the unfolding data.  
 $\ln k = \ln(k_F^{H_2O} \exp(-m_{\ddagger-U}[D]) + k_U^{H_2O} \exp(m_{\ddagger-F}[D] + m_{\ddagger-F}^*[D]^2))$ . Value in parentheses is  $m_{\ddagger-F}^*$ .  
<sup>c</sup> Calculated from kinetic data only,  $\beta_{\ddagger} = m_{\ddagger-U}/(m_{\ddagger-U} + m_{\ddagger-F})$ .  
<sup>d</sup> Calculated from kinetic and equilibrium data,  $\beta_{\ddagger} = 0.592 m_{\ddagger-U}/m_{U-F}$ .

To further verify the two-state model of folding for FKBP12, stopped-flow circular dichroism (CD) experiments were performed. Stopped-flow CD has been used extensively to detect burst phases in folding kinetics, i.e. a change in the ellipticity within the deadtime of the instrument, which can correspond to the rapid formation of an intermediate state with secondary structure. Figure 4 shows the kinetic trace obtained for a pH-jump initiated refolding experiment for FKBP12. The baseline was determined by rapid

(1:1) mixing of the pH-unfolded protein solution with unfolding buffer.

The absence of detectable intermediates on the folding pathway of a protein does not disqualify the possibility of unstable intermediate species. To test whether such an unstable intermediate state is present on the folding pathway of FKBP12, refolding experiments were performed in the presence of 0.4 M Na<sub>2</sub>SO<sub>4</sub>. The  $\ln k_F$  value remains linearly dependent on [urea] (Figure 3(a)).

**Table 3.** Comparison of thermodynamic parameters measured from equilibrium and kinetic experiments

Experiment	$\Delta G_{U-F}^{H_2O}$ <sup>a</sup>	Equilibrium $\Delta G_{U-F}^{H_2O}$ <sup>b</sup>	$m_{U-F}$ (kcal mol <sup>-1</sup> M <sup>-1</sup> )	Kinetic	
	(kcal mol <sup>-1</sup> ) $m_{U-F}$	(kcal mol <sup>-1</sup> ) $m_{U-F}$		$\Delta G_{U-F}^{H_2O}$ (kcal mol <sup>-1</sup> )	$m_{U-F}$ (kcal mol <sup>-1</sup> M <sup>-1</sup> )
<b>A. Urea</b>					
FKBP12	5.53 ± 0.12	6.15 ± 0.08	1.4 ± 0.03	5.8 ± 0.3	1.7 ± 0.5
<b>B. +TFE</b>					
+0% TFE	5.53 ± 0.12	6.15 ± 0.08	1.4 ± 0.03	5.9 ± 0.2	1.7 ± 0.6
+3.6% TFE	5.9 ± 0.3	7.0 ± 0.1	1.3 ± 0.07	6.9 ± 0.2	1.5 ± 0.6
+9.6% TFE	7.8 ± 0.4	7.3 ± 0.1	1.7 ± 0.09	7.7 ± 0.2	1.5 ± 0.7
+17% TFE	6.1 ± 0.2	5.80 ± 0.07	1.7 ± 0.04	6.4 ± 0.3	1.6 ± 0.7
<b>C. Temperature dependence</b>					
15°C				5.8 ± 0.3	1.8 ± 0.6
20°C				5.6 ± 0.2	1.7 ± 0.6
25°C				5.7 ± 0.2	1.7 ± 0.6
30°C				5.3 ± 0.2	1.7 ± 0.5
35°C				5.1 ± 0.3	1.6 ± 0.5
<b>D. GdnHCl</b>					
FKBP12	5.1 ± 0.2		6.6 ± 0.3	5.0 ± 0.1 6.1 ± 0.2 <sup>c</sup>	8.9 ± 0.2 ND <sup>d</sup>
+Rapamycin	8.2 ± 0.6		3.9 ± 0.3	7.0 ± 0.3	3.2 ± 0.1

<sup>a</sup> Calculated using equation (9) and the  $m_{U-F}$  value measured for that experiment.

<sup>b</sup> Calculated using equation 9 and an average  $m_{U-F}$  value of 1.59, see footnote to Table 1.

<sup>c</sup> Calculated from the best fit of the data to a two-state model using a second-order polynomial fit for the unfolding data,  $\ln k = \ln(k_F^{H_2O} \exp(-m_{\ddagger-U}[D]) + k_U^{H_2O} \exp(m_{\ddagger-F}[D] + m_{\ddagger-F}^*[D]^2))$ .

<sup>d</sup> Not determined due to the significant curvature in  $\ln k_U$  versus [GdnHCl].

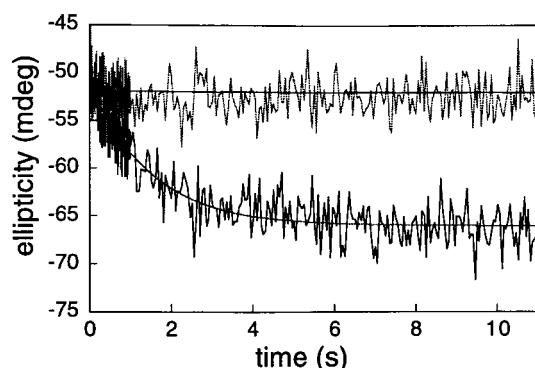


**Figure 4.** Stopped-flow circular dichroism experiment. The refolding reaction was initiated by pH jump. The kinetic trace is the average of 20 runs. Final conditions were 50 mM phosphate (pH 7.5), 1 mM DTT, 100  $\mu$ M FKBP12, 25  $^{\circ}$ C. The baseline was determined by 1:1 mixing of acid-unfolded FKBP12 with unfolding buffer, final conditions as above.

### Characterisation of the transition state of folding

#### *Compactness of the transition state: [denaturant]-dependence*

The values of  $m_{\ddagger-U}$  and  $m_{\ddagger-F}$  can be related to the average fractional change in degree of exposure of residues between initial and transition state in an analogous manner to  $m_{U-F}$  (Tanford, 1968, 1970). Thus, the ratio of  $m_{\ddagger-F}/m_{U-F}$  or  $m_{\ddagger-U}/m_{U-F}$  is a measure of the fractional change in degree of exposure of residues between the native or denatured state, and the transition state. A value  $\beta_T$  is defined as:

$$\beta_T = m_{\ddagger-U}/(m_{\ddagger-F} + m_{\ddagger-U}) \quad (6)$$

which is equivalent to  $1 - m_{\ddagger-F}/(m_{\ddagger-F} + m_{\ddagger-U})$  or  $m_{\ddagger-U}/m_{U-F}$  for a two-state system. Values for  $\beta_T$  calculated from urea and GdnHCl kinetic analyses are given in Table 2. The value of 0.7 is similar for both urea and GdnHCl experiments and within the range found for other proteins (Jackson, 1998).

#### *Structure of the ligand-binding site in the transition state*

The kinetics of unfolding and folding were determined as a function of denaturant concentration in the presence of the tight-binding ligand rapamycin (Figure 3(b)). The ligand concentration was in excess of the protein concentration such that, at the concentration used, all native FKBP12 was in the complexed form. As expected, the FKBP12-rapamycin complex unfolds many orders of magnitude slower than the uncomplexed protein. Although the exact difference in unfolding rate between free and complexed FKBP12 varies slightly with denaturant concentration, at 3.5 M GdnHCl the difference is greater than  $2 \times 10^5$ . In comparison,

there is relatively little effect on the folding rate (Figure 3(b)).

#### *Trifluoroethanol as a probe of secondary structure formation in the transition state*

Trifluoroethanol and other alcohols have recently been used to probe the extent of secondary structure formation in the transition state for folding of acyl phosphatase (AcP) (Chiti *et al.*, 1998, 1999). We performed similar experiments on FKBP12 in order to study the extent of helix formation in the transition state. The [urea]-dependence of the unfolding and refolding rate constants was measured at three different TFE concentrations, 3.6%, 9.6% and 17% (v/v). The results are shown in Figure 3(a). For all three TFE concentrations the data fit well to a two-state model, as shown by a comparison of the kinetic and equilibrium data (Table 3). Kinetic parameters obtained from the best fit of the data to a two-state model (equation (5)) are shown in Table 2. In 3.6 and 9.6% TFE the protein folds faster and unfolds more slowly than in the absence of TFE, consistent with the equilibrium results which show that low concentrations of TFE stabilise the native state relative to the unfolded state. In 17% TFE the protein folds faster but also unfolds faster than in the absence of TFE, consistent with the equilibrium results which show a slight destabilisation of the native state relative to the unfolded state under these conditions. Figure 3(c) shows the variation in the rate of unfolding and refolding with final TFE concentration. The folding rate increases with increasing concentrations of TFE up to a maximum rate enhancement of fourfold at 9.6% TFE, the refolding rate then decreases with increasing TFE concentration. This effect has also been observed for AcP (Chiti *et al.*, 1998, 1999). The unfolding rate increases with [TFE] in a manner similar to chemical denaturants. Extrapolation of the folding and unfolding rates into the transition region results in a crossover or midpoint of unfolding ( $k_U = k_F$ ) at approximately 30% TFE. Taking into account *cis-trans* proline isomerisation equilibria in the denatured state, this is consistent with the equilibrium experiments for which the midpoint was 26%.

To provide some measure of the extent of helix formation in the unfolded state of FKBP12 in the presence of TFE, far-UV circular dichroism spectra were recorded. Figure 5(a) shows the far-UV CD spectra of acid-unfolded FKBP12 in 0, 3.6 and 9.6% TFE, compared with the spectrum of the native protein (the spectrum of the native protein did not change with TFE, data not shown). At 9.6% TFE the helix content in the unfolded state is comparable to the native structure. The far-UV CD spectra of urea-unfolded, native and TFE-unfolded FKBP12 demonstrate that there is extensive non-native helix formation at 40% (Figure 5(b)).

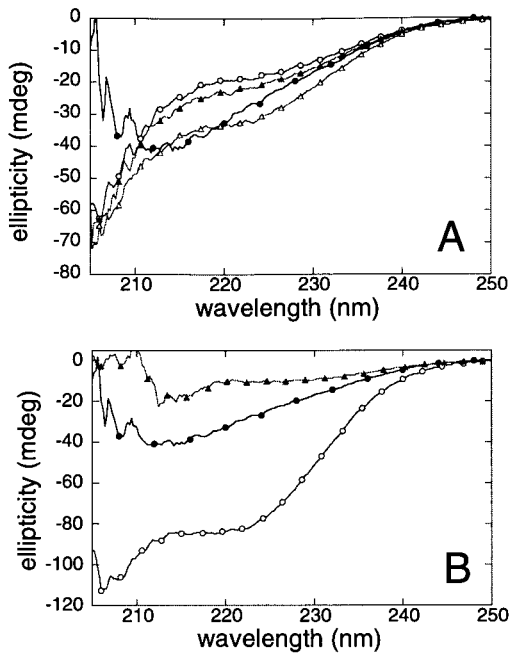


**Figure 5.** Circular dichroism spectra. (a) Far-UV circular dichroism spectra of native wild-type FKBP12 in 50 mM phosphate (pH 7.5), 1 mM DTT (filled circles), acid-unfolded FKBP12 (32 mM HCl, 1 mM DTT) in 0% TFE (open circles), 3.6% TFE (filled triangles) and 9.6% TFE (open triangles). FKBP12 was 33  $\mu$ M, pathlength was 2 mm. (b) Far-UV spectra of native FKBP12 (50 mM phosphate (pH 7.5), 1 mM DTT) (filled circles), acid-unfolded FKBP12 (32 mM HCl, 1 mM DTT) (filled triangles) and TFE-unfolded FKBP12 (50 mM phosphate (pH 7.5), 1 mM DTT, 40% TFE) (open circles). FKBP12 was 33  $\mu$ M, pathlength was 2 mm.

#### Thermodynamic nature of the transition state: temperature-dependence studies

Unfolding and refolding rates were measured as a function of urea concentration at five different temperatures (Table 4). Over the temperature range 15–35  $^{\circ}$ C the folding of FKBP12 remains two-state (Figure 6(a)). The rate constant for unfolding was also measured over a wider range of temperatures at a single final urea concentration (7 M). The Eyring plot for these data is shown in Figure 6(b) and is clearly non-linear. Non-linearity in Eyring plots is observed when there is a significant difference in the heat capacity between the initial state and the transition state. In this case  $\Delta H^{\ddagger}$ , the activation enthalpy, and thus  $\Delta G^{\ddagger}$ , the activation energy, are dependent on temperature. Following the analysis by Chen *et al.* (1989), the data can be fitted to:

$$\ln \frac{k_U}{T} = A + B \frac{T_0}{T} + C \ln \frac{T_0}{T} \quad (7)$$

where:

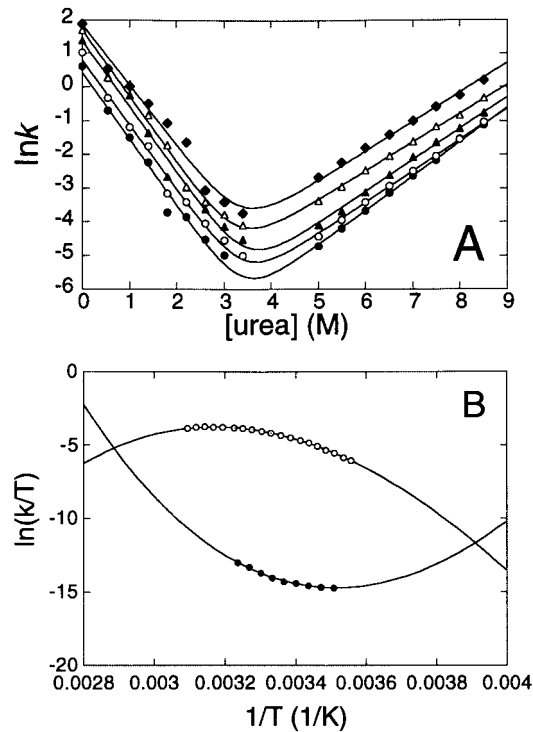


**Figure 6.** Temperature-dependence of the rate constants for unfolding and refolding. (a) The [urea]-dependence of the natural logarithm of the rate constants for unfolding and refolding of FKBP12 at 15  $^{\circ}$ C (filled circles), 20  $^{\circ}$ C (open circles), 25  $^{\circ}$ C (filled triangles), 30  $^{\circ}$ C (open triangles) and 35  $^{\circ}$ C (filled diamonds). Rate constants are measured in 50 mM phosphate (pH 7.5), 1 mM DTT. The continuous curves shows the best fit of the data to a two-state model (equation (5)). (b) Eyring plot of the temperature dependence of the unfolding rate constant at a final urea concentration of 7 M, in 50 mM phosphate (pH 7.5), 1 mM DTT (filled circles). The continuous curve shows the best fit of the data to equation (7). The data shown have been offset by a constant in order to illustrate the unfolding and refolding curves under identical conditions, i.e. in water. The data were not offset when fitting to equation (7). Eyring plot of the temperature dependence of the fast refolding rate constant at 0 M urea, in 50 mM phosphate (pH 7.5), 1 mM DTT (open circles). The continuous curve shows the best fit of the data to equation (7). The intersects of the two curves indicate the point at which the midpoint of heat or cold denaturation, and are +73  $^{\circ}$ C and -17  $^{\circ}$ C, respectively.

$$A = \frac{[-\Delta C_p^{\ddagger} + \Delta S^{\ddagger}(T_0)]}{R} - \ln \frac{h}{k_B}$$

$$B = \frac{[\Delta C_p^{\ddagger} - \Delta S^{\ddagger}(T_0)]}{R} - \frac{\Delta G^{\ddagger}(T_0)}{RT_0}$$

$$C = -\frac{\Delta C_p^{\ddagger}}{R}$$

and where  $\Delta C_p^{\ddagger}$  is the heat capacity change between the initial and transition state,  $\Delta S^{\ddagger}$  is the



**Table 4.** Kinetic parameters for the temperature dependence of the refolding and unfolding rate constants

	$k_{\text{U}}^{\text{H}_2\text{O}}$ ( $\text{s}^{-1}$ )	$m_{\ddagger\text{-F}}^{\text{a}}$ ( $\text{M}^{-1}$ ) <sup>a</sup>	$k_{\text{F}}^{\text{H}_2\text{O}}$ ( $\text{s}^{-1}$ )	$m_{\ddagger\text{-U}}^{\text{a}}$ ( $\text{M}^{-1}$ ) <sup>a</sup>	$\beta_{\text{T}}^{\text{b}}$
15°C	1.53 ± 0.22	1.98 ± 0.08	5.66 ± 2.40	1.02 ± 0.06	0.7
20°C	2.22 ± 0.26	1.93 ± 0.07	12 ± 4.2	0.93 ± 0.05	0.7
25°C	3.93 ± 0.51	1.95 ± 0.07	16.2 ± 6.2	0.94 ± 0.06	0.7
30°C	5.44 ± 0.72	1.97 ± 0.08	49 ± 18	0.85 ± 0.05	0.7
35°C	6.45 ± 0.98	1.81 ± 0.09	78 ± 33	0.88 ± 0.06	0.7

<sup>a</sup> To convert to  $\text{kcal mol}^{-1} \text{M}^{-1}$ , the same unit as the  $m_{\text{U-F}}$ , multiply by a factor of RT.

<sup>b</sup>  $\beta_{\text{T}} = m_{\ddagger\text{-U}} / (m_{\ddagger\text{-F}} + m_{\ddagger\text{-U}})$ .

change in entropy between initial and transition state,  $\Delta H^\ddagger$  is the change in enthalpy between initial and transition state, and  $\Delta G^\ddagger$  is the change in free energy between initial and transition state. The activation parameters for unfolding and refolding of FKBP12 are shown in Table 5. Subscript U is used to denote the activation parameters for the unfolding reaction and subscript F is used to denote the activation parameters for the refolding reaction.

The temperature dependence of the fast refolding phase was determined by pH-jump experiments over the temperature range 8–48°C. The Eyring plot shows significant curvature over this temperature range (Figure 6(b)). As with the unfolding data, this curvature results from a significant change in heat capacity on going from the denatured state to the transition state. The data were analysed using equation (7), and the activation parameters calculated are shown in Table 5.

### Characterisation of the slow refolding phases

Slow phases are often observed in refolding reactions due to the heterogeneous nature of the denatured state resulting from *cis-trans* proline isomerisations (Brandts *et al.*, 1975; Kim & Baldwin, 1982). Two slow refolding phases are observed for FKBP12 (see Figure 7(a)). Previous studies have shown that the slowest phase is limited by a proline isomerisation step (Scholz *et al.*, 1996; Veeraghavan *et al.*, 1996). Here we show that the second refolding phase, observed only at low concentrations of denaturant, is also due to proline isomerisation. Refolding experiments were performed in the presence of the peptidyl-prolyl isomerase (PPIase), cyclophilin A. At high concentrations of cyclophilin A both slow phases are accelerated sufficiently that a single exponential process is observed (see Figure 7(a)). Double-jump experiments were also performed. Using a delay time of

100 ms (between unfolding and refolding) the slowest phase disappears, consistent with evidence that it is due to a slow rate-limiting proline isomerisation event (Figure 7(b)). The faster of the two slow phases, however, is still observed. Although, this is not consistent with the rates of *trans-cis* proline isomerisation measured for model proline-containing peptides (Grathwohl & Wuthrich, 1981), several groups have observed fast proline isomerisations in proteins (Jackson & Fersht, 1991b; Schmid *et al.*, 1996). Further, double-jump experiments in the presence of cyclophilin A, (Figure 7(b)) show that this phase can be catalysed by PPIases, and at sufficiently high concentrations of cyclophilin A, a single exponential is again observed (Figure 7(b)).

## Discussion

### Evidence for a two-state transition

It has previously been shown that FKBP12 unfolds according to a two-state model under equilibrium conditions (Egan *et al.*, 1993). Here, we show that FKBP12 also folds according to a two-state model under non-equilibrium conditions, i.e. no intermediates are significantly populated on the unfolding or refolding pathway of this protein even in the absence of denaturant. Two pieces of evidence suggest this. First, the plots of  $\ln k_{\text{U}}$  and  $\ln k_{\text{F}}$  versus [urea] are linear, resulting in the characteristic V-shaped curves shown in Figure 3(a). In this case linearity is an indication, but not proof, that the protein folds by a two-state mechanism. Second, and most important, data obtained from kinetic experiments can be compared to equilibrium data. Values for  $\Delta G_{\text{U-F}}^{\text{H}_2\text{O}}$  and  $m_{\text{U-F}}$  calculated from the kinetic data, assuming a two-state transition, are within experimental error of the values obtained directly from equilibrium experiments (Table 3). Stopped-flow CD experiments provide

**Table 5.** Activation parameters for the refolding and unfolding of FKBP12 calculated from the Eyring plots

	$\Delta C_{\text{p}}^\ddagger$ ( $\text{kcal mol}^{-1} \text{K}^{-1}$ )	$\Delta G^\ddagger$ (298 K) ( $\text{kcal mol}^{-1}$ )	$\Delta S^\ddagger$ ( $\text{cal mol}^{-1} \text{K}^{-1}$ )	$\Delta S^\ddagger$ (298 K) ( $\text{kcal mol}^{-1}$ )	$\Delta H^\ddagger$ (298 K) ( $\text{kcal mol}^{-1}$ )
Unfolding	1.04 ± 0.08	18.7 ± 0.01	−16 ± 1	−4.7 ± 0.3	14 ± 0.3
Refolding	−0.67 ± 0.01	16.6 ± 0.01	−17 ± 0.2	−5.0 ± 0.07	11.6 ± 0.07

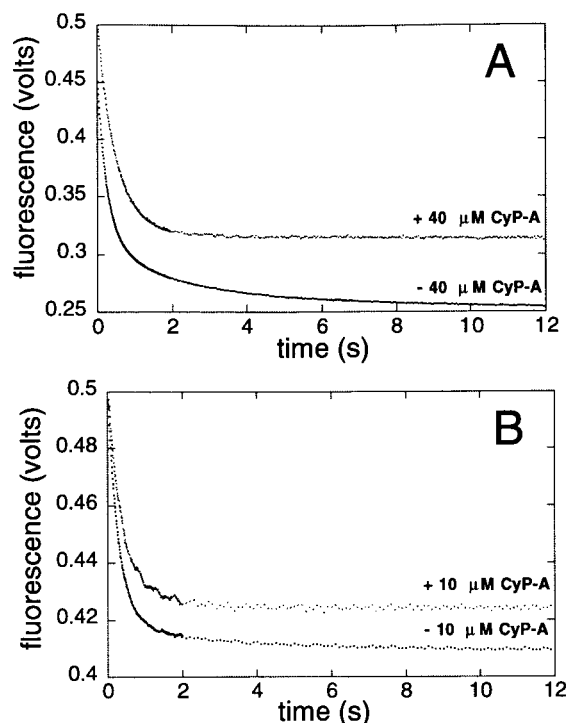


**Figure 7.** Characterisation of the slow refolding phases. (a) Kinetic trace for the refolding of FKBP12 in 50 mM Tris-HCl (pH 7.5), 1 mM DTT at 25°C in the absence and presence of 40  $\mu\text{M}$  cyclophilin A (CyP-A). The first trace can be fitted to a triple exponential, whereas the second trace (+ cyclophilin A) can be fitted to a single exponential process with residuals <1%. (b) Double-jump stopped-flow fluorescence experiment. Delay time was 100 ms. Kinetic traces, in the absence and presence of 10  $\mu\text{M}$  cyclophilin A, CyP-A. The first trace (-CyP-A) can be fitted to a double exponential process (residuals <1%) whereas the second trace (+CyP-A) can be fitted to a single exponential process with residuals <2%.

further evidence. Even in the absence of denaturant, no burst phase is observed during the refolding of FKBP12, as monitored by the far-UV CD signal at 222 nm (Figure 4).

For other proteins, high energy intermediates have been detected by changing the conditions such that the intermediate state is stabilised relative to the unfolded state. This has been achieved, in the case of ubiquitin, by the addition of  $\text{Na}_2\text{SO}_4$  (Khorasanizadeh *et al.*, 1996), and for acylphosphatase by the addition of trifluoroethanol (Chiti *et al.*, 1998). In these cases, the observed kinetics become three-state. By comparison, the folding of FKBP12 remains two-state on addition of 0.4 M  $\text{Na}_2\text{SO}_4$  or 17% TFE (v/v) (Figure 3(a)). This suggests that either FKBP12 folds without intermediate states, or that, if present, these intermediate states are very high in energy and/or only very transiently populated compared with other conformations.

## Comparison with other proteins

There are now at least 20 proteins which have been reported to fold with two-state kinetics (Jackson, 1998). For some of these proteins, however, the folding rate has not been measured in the absence of denaturant, so one cannot rule out the presence of stable intermediate states in water. The difficulties in measuring the folding rate in water may result from the fact that not all proteins denature at low pH, or that the folding rates are too fast to measure by conventional stopped-flow techniques.

Most proteins that fold with two-state kinetics are small, typically less than 90 residues and often between 60 and 80 residues in length. It has been proposed that the larger the protein, the more likely it will exhibit non-two-state behaviour (Fersht, 1995), so it is interesting to note that, despite its size, FKBP12 still follows two-state kinetics. In fact, several smaller proteins exhibit more complex kinetics including ubiquitin (76 residues, Khorasanizadeh *et al.*, 1996) and barstar (89 residues, Schreiber & Fersht, 1993).

For proteins which fold with two-state kinetics there is a wide spread in the observed, or extrapolated, folding rate in water; the slowest is muscle acyl phosphatase with a  $k_{\text{F}}^{\text{H}_2\text{O}}$  of  $0.23 \text{ s}^{-1}$  at 25°C (van Nuland *et al.*, 1998), and the fastest a mutant of monomeric  $\lambda$  repressor with a rate of  $88,000 \text{ s}^{-1}$  at 37°C (Burton *et al.*, 1996). In comparison to many other proteins, FKBP12 is quite slow to fold. This raises some interesting questions about the nature of the kinetic barriers to folding. In order to address this and other questions we have characterised the transition state for folding using a number of complementary techniques and approaches. Here we have used four different experiments on the wild-type protein to characterise the transition state. In the accompanying paper we present studies using protein engineering techniques and  $\Phi$ -value analysis to characterise the energetics of the transition state, as well as presenting structures of the transition state obtained directly from molecular dynamic simulations (Fulton *et al.*, 1999).

## Characterisation of the transition state of folding

### Compactness

Kinetic experiments are the only experimental method for obtaining information on the nature of transition states, whether it be in a simple chemical reaction or in a complex reaction such as protein folding. Using approaches based in physical organic chemistry, perturbations to the system and their effect on the kinetics and equilibrium of a process can be used to inform on the nature of the transition state. For the wild-type protein we have used perturbations in denaturant concentration, temperature, ligand concentration, and solvent. We have measured the effects of these on the kinetics

of folding and unfolding and compared these to their effects on the unfolding equilibrium.

The value of  $\beta_T$  is a measure of the average exposure of residues in the transition state relative to the unfolded and native states. The value for FKBP12 is 0.7, indicating that, on average, 70 % of the surface area buried in the native structure is already buried in the transition state and that the transition state is a compact state relative to the unfolded state. Even for simple two-state systems  $\beta_T$  is highly variable (Jackson, 1998). The highest reported value, indicating that the transition state is close to the native state, is 0.9 for the cold shock family of proteins (Schindler *et al.*, 1995), whereas the lowest value is 0.4-0.5, for wild-type monomeric  $\lambda$  repressor (Burton *et al.*, 1996), and cytochrome *c* (Chan *et al.*, 1997; Mines *et al.*, 1996). The value for FKBP12 is typical of many other proteins.

Changes in heat capacity between the denatured, transition and native state, calculated from temperature-dependence studies (Chen *et al.*, 1989) can also be used as a measure of the compactness of the transition state. A  $\beta_T$  (heat capacity) value can be defined as  $\Delta C_{pF}^{\ddagger}/(\Delta C_{pF}^{\ddagger} - \Delta C_{pU}^{\ddagger})$ . (The main contribution to heat capacity is from hydrophobic residues, so the ratio reflects the degree to which hydrophobic side-chains have become buried in the transition state relative to the denatured state.) For FKBP12,  $\beta_T$  (heat capacity) is 0.4, which is substantially lower than the value obtained from *m*-values. Differences in  $\beta_T$  measured from [denaturant]-dependence experiments and temperature-dependence experiments has been noted elsewhere (Plaxco & Baker, 1998). Molecular dynamic simulations (see the accompanying paper) suggest the structural basis for this result: the total accessible surface area increases by 30-37 % in the transition state, whereas the non-polar side-chain surface area increases by 50-55 % (Fulton *et al.*, 1999).

### Thermodynamics

Table 5 summarises the thermodynamic parameters for the transition state relative to the unfolded or native state obtained from the temperature-dependence studies. There is a large enthalpic contribution to the unfolding and refolding activation energy at 298 K, and a much smaller entropic contribution. In general it is difficult to interpret changes in enthalpy and entropy as the factors contributing to these terms are complex and include solvation effects. The activation enthalpy for unfolding is large and positive, as has been observed for other proteins, and is attributed to the loss of favourable interactions present in the native state. The large, positive activation enthalpy for folding can be attributed to the formation of hydrophobic interactions in the transition state. It is interesting to note that the activation entropies for unfolding and refolding are both small and negative. Values for  $\Delta S_{\ddagger}^{\ddagger}$  are frequently negative, a result of the decrease in chain entropy. Negative values for  $\Delta S_{U}^{\ddagger}$ , however, are less common, and

indicate a decrease in entropy between native and transition state. For FKBP12 this may result from the increase in solvent accessibility of hydrophobic side-chains in the transition state, forcing water molecules to order around exposed hydrophobic groups.

### Ligand-binding site

The binding of ligands and the energetics of ligand-protein interactions can be used to probe the extent of structure formation in ligand-binding sites in the transition state for folding (Sancho *et al.*, 1992). Here we have used the tight-binding ligand rapamycin to probe the ligand-binding site in the transition state for folding of FKBP12. Rapamycin binds tightly to the native state of FKBP12, thus stabilising it towards chemical denaturation, and a large shift in the midpoint of denaturation is observed (Figure 2(a)). The effect of rapamycin on the unfolding rate suggests that the ligand-binding site is only very weakly formed in the transition state. It is interesting to note that there is some effect on the folding kinetics and this is under further investigation.

### Secondary structure in the transition state

Alcohols such as trifluoroethanol and hexafluoroisopropanol have been reported to accelerate the rate of folding of hen lysozyme and acyl phosphatase (Chiti *et al.*, 1998, 1999; Lu *et al.*, 1997). For hen lysozyme these results have been attributed to a weakening of hydrophobic interactions with increasing TFE, which destabilises a misfolded species on the folding pathway which acts as a kinetic trap. For acyl phosphatase, however, the acceleration in folding rate has been attributed to changes in the stability of native  $\alpha$ -helices in the denatured state. It is argued that formation of native  $\alpha$ -helices in the denatured state leads to an increase in rate on entropic grounds, as there is no unfavourable loss in entropy on forming the helix in the transition state (Chiti *et al.*, 1998). The maximum rate enhancement (20-fold) is obtained at a TFE concentration where far-UV CD spectra indicate a native amount of  $\alpha$ -helix in the denatured state. At concentrations greater than this, the folding rate decreases as non-native helices are stabilised. We find very similar results for FKBP12, a rate enhancement of fourfold is observed at 9.6 % TFE, the concentration at which the helical content of the acid-unfolded state is comparable to the native state (Figure 5(a)). This finding suggests that the  $\alpha$ -helix may be formed in the folding transition state.

In comparison, to the results on acyl phosphatase no "rollover" was observed in the plots of  $\ln k_F$  versus [D] for high concentrations of TFE (Figure 3(d)), indicating that even at high concentrations of TFE, where non-native helices are present in the denatured state, intermediates do not accumulate on the folding pathway.

### *Nature of the transition state and comparison with protein engineering studies and molecular dynamics simulations*

Together these results suggest a compact transition state relative to the unfolded state, where some 70 % of the surface area has become inaccessible to solvent. Approximately 30 % of the hydrophobic surface area is still accessible to solvent in the transition state, which may account for the observed negative entropy of activation of unfolding. Protein engineering and molecular dynamic studies have provided more detailed information on the burial of hydrophobic residues (Fulton *et al.*, 1999). Together these studies have shown that some regions of the protein are more highly structured in the transition state than others, indicating that a non-specific hydrophobic collapse cannot have occurred. It is interesting to note that, although there has been a significant burial of hydrophobic residues, no residues investigated so far have  $\Phi$ -values greater than 0.6. Although partially secluded from solvent, the side-chains have not achieved the tight packing characteristic of the native state.

Ligand-binding studies show that the ligand-binding site is largely unstructured in the transition state. In structural terms these results suggest that  $\beta$ -strand 3, the loop connecting  $\beta$ -strand 3 and the  $\alpha$ -helix, and the 80 s loop which forms the ligand-binding site, are largely unstructured in the transition state. The TFE experiments suggest that the  $\alpha$ -helix may be formed in the transition state, at least in the presence of TFE. This finding is in disagreement with protein engineering and molecular dynamics studies which indicate that only the C-terminal region of the helix is weakly formed in the transition state and that the N terminus of the helix is largely unstructured (Fulton *et al.*, 1999). Such a discrepancy could arise if TFE changes the pathway of folding, favouring pathways in which the helical structure is formed early, or if TFE has a global effect on protein structure and not a specific effect on the  $\alpha$ -helix. This problem has been addressed by performing a  $\phi$ -value analysis in water and in TFE. The results from these studies suggest that TFE acts globally on the protein and does not stabilise any single element of secondary structure (Main & Jackson, 1999).

## Conclusions

We have shown that the 107-residue FKBP12 protein folds with simple two-state kinetics in water. It folds efficiently without populating intermediate states or misfolded species which could act as kinetic traps. Thus, both its size and structure, which includes the topological crossing of two loops, do not prevent it from folding with a simple two-state mechanism. The transition state is relatively compact compared to the unfolded state,

but some hydrophobic side-chains are exposed to solvent suggesting a weakening of the hydrophobic core. Some regions of the protein, such as the loops involved in ligand binding, are not structured in the transition state. In general there is good agreement between these studies and the results of protein engineering and molecular dynamic simulations reported by Fulton *et al.* (1999).

## Materials and Methods

### Materials

Isopropyl-thio- $\beta$ -D-galactoside (IPTG) was purchased from HT-Technologies or Sigma. Ultra-grade urea was used (Fisher Scientific UK Ltd.) and guanidinium chloride was purchased from Fluka Biochemika. Glutathione agarose was from Pharmacia or Sigma. All other materials were analytical grade and purchased from Sigma.

### Construction of pGST-FKBP12 expression vector

The glutathione-S-transferase (GST) gene fragment from pGEX-2T (Pharmacia) was amplified with *Nco*I and *Bam*HI restriction sites using standard polymerase chain reaction techniques. This fragment was subcloned into a pTrcHis-A vector (Invitrogen) which had been modified to remove the histidine tag. This created a new GST-fusion vector (pTrcGST) which is under the control of the *trc* promoter and is IPTG-inducible. The wild-type human FKBP12 gene was amplified with *Bam*HI and *Eco*RI restriction sites and subcloned into the multiple-cloning site of the pTrcGST vector to create a new high-level expression vector, pGST-FKBP12.

### Expression and purification of recombinant human FKBP12

An overnight culture of *Escherichia coli* BL21 cells harbouring the pGST-FKBP12 plasmid was used to inoculate a large volume of LB broth containing 50  $\mu$ g ml<sup>-1</sup> ampicillin. This was grown at 37°C with shaking for two to three hours until the absorption of the cells at 600 nm was 0.5-1.0. IPTG was added to a final concentration of 0.1 mM to induce expression of the GST-FKBP12 fusion protein, and the temperature reduced to 30°C to minimise inclusion body formation. Cells were harvested after three hours by centrifugation in a large (SLA-3000) Sorvall rotor for ten minutes at 5000 rpm at 4°C. The cell pellet was resuspended in 30 ml of ice-cold PBS (~30 ml per ~10 g of whole cell pellet) containing ~1 mg ml<sup>-1</sup> lysozyme and kept on ice for 30 minutes. Cells were then freeze-thawed four times using liquid nitrogen and a 37°C water-bath and then sonicated (6 × 20 seconds, 4°C) to ensure complete lysis. Triton-X-100 was added to a final concentration of 1% (v/v) and the mixture left for 30 minutes on ice. Cell debris was removed by centrifugation at 18,000 rpm in a Sorvall SS-34 rotor for one hour at 4°C and the supernatant was filtered and loaded onto a PBS-equilibrated gravity flowing glutathione-agarose column. The GST-FKBP12 fusion protein was eluted with 50 mM Tris (pH 7.5), 10 mM reduced glutathione and then cleaved overnight at room temperature with thrombin. Separation of FKBP12 from the GST and thrombin was achieved using a Pharmacia

HiLoad FPLC G75 Superdex column (26/60) which had been pre-equilibrated with 50 mM Tris (pH 7.5), 150 mM NaCl. DTT (1 mM) was added to prevent oxidation of the cysteine residue. Purified protein was then concentrated, flash-frozen and stored in liquid nitrogen or at  $-80^{\circ}\text{C}$ . The purity of the protein was determined using SDS/polyacrylamide gel electrophoresis and mass spectroscopy. Protein concentration was determined spectrophotometrically using a molar extinction coefficient,  $\epsilon$ , of  $9927\text{ M}^{-1}\text{ cm}^{-1}$  at 278 nm (Egan *et al.*, 1993).

### Equipment and general procedures

In all the equilibrium and kinetic experiments the final buffer concentration was 50 mM Tris-HCl (pH 7.5), 1 mM DTT, except the temperature dependence studies where 50 mM phosphate (pH 7.5), 1 mM DTT was used. All stock solutions of urea or guanidinium chloride (GdnHCl) were made using volumetric flasks, and the urea solutions were flash-frozen and stored at  $-20^{\circ}\text{C}$  to prevent degradation. All protein solutions were filtered ( $0.2\ \mu\text{m}$  Sartorius Minisart filter) prior to addition to denaturant solutions.

### Equilibrium experiments

#### *Urea and guanidinium chloride denaturation: preparation of samples*

A stock solution of urea (8–10 M) or GdnHCl (2–8 M), was diluted to obtain a large range of denaturant concentrations using a Hamilton Microlab dispenser; 100  $\mu\text{l}$  of a stock solution of FKBP12 (ca 18–36  $\mu\text{M}$ ) containing 450 mM Tris-HCl (pH 7.5), 9 mM DTT was added to each denaturant sample (800  $\mu\text{l}$ ). For the 3.64% TFE experiment the stock FKBP12 solution was as above, with the addition of TFE to 32.8% (v/v). For the experiments at 9.6% and 17% TFE, TFE was added to the individual denaturant solutions. The protein/denaturant solutions were pre-equilibrated at  $25^{\circ}\text{C}$  for at least one hour. The GdnHCl-denaturation of the FKBP12-rapamycin complex followed the same procedure, except that 18  $\mu\text{l}$  of a stock solution of rapamycin (1 mM in ethanol) and 82  $\mu\text{l}$  of a stock solution of FKBP12 (22  $\mu\text{M}$ ) containing 549 mM Tris-HCl (pH 7.5), 11 mM DTT was added to each 800  $\mu\text{l}$  GdnHCl sample to give final concentrations of FKBP12 and rapamycin of 2 and 20  $\mu\text{M}$ , respectively. The FKBP12-rapamycin-denaturant solutions were pre-equilibrated at  $25^{\circ}\text{C}$  for ca 24 hours.

#### *TFE denaturation*

TFE (100%, v/v) was split and diluted to obtain a large range of TFE concentrations using a Hamilton Microlab dispenser. A 100  $\mu\text{l}$  portion of a FKBP12 stock solution (18–36  $\mu\text{M}$  FKBP12, 450 mM Tris-HCl (pH 7.5), 9 mM DTT) was added to each TFE sample (800  $\mu\text{l}$ ). The protein/TFE solutions were pre-equilibrated at  $25^{\circ}\text{C}$  for at least one hour.

### Spectroscopic measurements

All measurements were performed in a thermostatted cuvette holder at  $25^{\circ}\text{C}$  using either a Perkin Elmer Luminescence Spectrometer LS50B, or a SLM Aminco Bowman Series 2 Luminescence Spectrometer. The excitation wavelength was 280 nm, and band passes for excitation

and emission typically 2.5–10 nm. The fluorescence of FKBP12 was measured at the  $\lambda_{\text{max}}$  for the denatured state, either 356 nm for FKBP12 or FKBP12-rapamycin experiments, or 347 nm for experiments in the presence of TFE.

### Kinetic experiments

An Applied Photophysics Stopped Flow Reaction Analyser (model SF.17MV) was used and data were acquired and analysed using the Applied Photophysics Kinetic Workstation, version 4.099, supplied. In all studies the temperature was  $25(\pm 0.1)^{\circ}\text{C}$ , unless otherwise stated.

### Unfolding studies

Unfolding was performed by [denaturant] or [TFE]-jump experiments in the following manner. Unfolding was initiated by diluting one volume of an aqueous protein solution (ca 22  $\mu\text{M}$  FKBP12 in 50 mM Tris-HCl (pH 7.5), 1 mM DTT) into ten volumes of either concentrated denaturant or TFE solution (containing 50 mM Tris-HCl (pH 7.5), 1 mM DTT) such that the final concentrations were between 3.5 and 8.5 M for urea, 1 and 3.5 M for GdnHCl, and 40–80% for TFE. For the urea-induced unfolding experiments in the presence of TFE both aqueous native protein solution and unfolding buffer contained 3.64% or 9.6% TFE.

For the GdnHCl-induced unfolding of the FKBP12-rapamycin complex a stock solution of FKBP12 (22  $\mu\text{M}$ ) and rapamycin (44  $\mu\text{M}$ ) was pre-equilibrated in 50 mM Tris (pH 7.5), 1 mM DTT. Unfolding was then initiated by manually mixing one volume of the aqueous protein/rapamycin solution into ten volumes of concentrated GdnHCl, final concentrations varying between 3.5 and 5 M. Under these conditions unfolding is sufficiently slow that manual mixing can be employed and the reaction followed SLM Aminco Bowman Series 2 Luminescence Spectrometer.

### Refolding studies

Refolding was initiated by either [denaturant], [TFE] or pH-jump experiments.

#### *[Denaturant]-jump*

Protein was initially unfolded in 50 mM Tris-HCl (pH 7.5), 1 mM DTT containing either 6.0 M urea, 1.2 M GdnHCl or 40% (v/v) TFE. Refolding was then initiated by rapid mixing of one volume of denatured protein into ten volumes of a refolding buffer containing 50 mM Tris-HCl (pH 7.5), 1 mM DTT, and appropriate amounts of denaturant or TFE to give final concentrations between 0.54 and 3.5 M urea, 0.11 and 0.6 M GdnHCl, or 3.64 and 17% TFE. [Urea]-jump experiments were also performed in the presence of small amounts of TFE by the addition of either 3.64% or 9.6% TFE to both the urea-unfolded protein solution and the refolding buffers. [GdnHCl]-jump refolding experiments were also performed on the FKBP12-rapamycin complex. The complex (22  $\mu\text{M}$  FKBP12, 44  $\mu\text{M}$  rapamycin, 50 mM Tris-HCl (pH 7.5), 1 mM DTT) was initially unfolded in 3 M GdnHCl. Refolding was then initiated by manual or rapid mixing of one volume of the denatured protein/rapamycin solution into ten volumes of a refolding buffer. Final GdnHCl concentrations were between 0.27 and 1.4 M.

### pH-jump (alkali and acid)

Protein was initially denatured by changing the pH to either 1.5 (by addition of 5 M HCl to give a final concentration of 32 mM) or 12 (by addition of NaOH to give a final concentration of 10 mM). The protein was refolded by rapid mixing (1:1) with refolding buffer containing either 100 mM Tris-HCl (pH 8.1), 1 mM DTT for acid-jump or 100 mM Tris-HCl (pH 7.2), 1 mM DTT for the alkali-jump. In both cases, the final solution was 50 mM Tris-HCl (pH 7.5), 1 mM DTT. The pH-jump experiments were performed in the absence and presence of low concentrations of denaturants and TFE.

### Double-jump experiments

Native protein, weakly buffered in 1 mM Tris-HCl (pH 7.5), 1 mM DTT, was rapidly denatured by a 1:1 dilution into unfolding buffer containing 64 mM HCl. Delay times between 0.1 and 10 seconds were used before the protein was then rapidly mixed (1:1) with a refolding buffer containing 100 mM Tris-HCl (pH 8.1), 1 mM DTT (to give a final solution of 50 mM Tris-HCl (pH 7.5), 1 mM DTT). This was achieved using an Applied Photophysics Stopped Flow Reaction Analyser (model SF.17MV) in double-jump mode. Under these conditions FKBP12 unfolds within the deadtime of the instrument (<10 ms).

### Refolding in the presence of cyclophilin A

pH-jump and double-jump experiments, as described above, were also performed in the presence of 0-50  $\mu$ M cyclophilin A. Human cyclophilin A was expressed as a fusion protein with GST and purified as described for FKBP12. The concentration of cyclophilin A was determined spectrophotometrically using a molar extinction coefficient,  $\epsilon$ , of 25,900 M<sup>-1</sup> cm<sup>-1</sup> at 280 nm.

### Circular dichroism spectroscopy

Far-UV CD spectra were acquired using a Jasco J-720 spectropolarimeter with thermostatted cuvette holder. Native protein samples were 33  $\mu$ M FKBP12 in 50 mM phosphate (pH 7.5), 1 mM DTT. TFE (100%) was added to give final concentrations of 0, 3.6, 9.6, 17% (v/v). Acid-denatured samples were prepared by the addition of 5 M HCl to an unbuffered protein sample to give a final concentration of 32 mM HCl (pH 1.5). The protein concentration was 33  $\mu$ M, DTT was added to a final concentration of 1 mM, and TFE added as above. A TFE-denatured sample was prepared by the addition of 100% TFE to 33  $\mu$ M FKBP12 in 50 mM phosphate (pH 7.5), 1 mM DTT, to give a final concentration of 40% (v/v). A 2 mm pathlength cell was used.

### Stopped-flow circular dichroism spectroscopy

An Applied Photophysics Stopped-flow was used in 1:1 mixing mode. The reaction was followed at 222 nm with a band pass of 10 nm, and a pathlength of 2 mm. The refolding reaction was initiated by pH jump as described above, but a 100 mM phosphate (pH 8.1), 1 mM DTT solution was used (final concentration 50 mM (pH 7.5), 1 mM DTT). Protein concentrations were 100  $\mu$ M after mixing.

### Equilibrium data analysis: Calculation of $[D]_{50\%}$ and $m_{U-F}$

The entire data set from the fluorescence monitored denaturation experiments can be fitted to equation (8) using the non-linear regression analysis program Kaleidagraph (version 3.0 Synergy Software, PCS Inc.):

$$F = \frac{\alpha_N + \beta_N[D] + (\alpha_U + \beta_U[D]) \exp(m_{U-F}([D] - [D]_{50\%})/RT)}{1 + \exp(m_{U-F}([D] - [D]_{50\%})/RT)} \quad (8)$$

where  $F$  is the observed fluorescence,  $\alpha_N$  and  $\alpha_U$  are the intercepts, and  $\beta_N$  and  $\beta_U$  are the slopes of the baselines at the low (N) and high (U) denaturant concentrations,  $[D]_{50\%}$  is the midpoint of unfolding,  $[D]$  is the concentration of denaturant and  $m_{U-F}$  is a constant that is proportional to the increase in degree of exposure of the protein on denaturation. Equation (8) is based on a two-state model of denaturation where only the native and the denatured states are populated, and assumes that the fluorescence of the native state,  $F_N$ , and the denatured state,  $F_U$ , are linearly dependent on the denaturant concentration ( $F_N = \alpha_N + \beta_N[D]$ ,  $F_U = \alpha_U + \beta_U[D]$ ); for a detailed derivation see Jackson & Fersht (1991a). Values for  $[D]_{50\%}$  and  $m_{U-F}$  are obtained with their standard errors.  $\Delta G_{U-F}^{H_2O}$ , the free energy of unfolding in water, can also be calculated using equation (9):

$$\Delta G_{U-F}^{H_2O} = m_{U-F}[D]_{50\%} \quad (9)$$

### Acknowledgements

S.E.J. is a Royal Society University Research Fellow, E.R.G.M. is supported by a BBSRC studentship, K.F.F. is supported by an Elmore Scholarship, Gonville & Caius College, Cambridge. We are grateful to Professor Steve Ley for kindly providing rapamycin.

### References

- Ahmad, F. & Bigelow, C. C. (1986). Estimation of the stability of globular-proteins. *Biopolymers*, **25**, 1623-1633.
- Bierer, B. E., Mattila, P. S., Standaert, R. F., Herzenberg, L. A., Burakoff, S. J., Crabtree, G. & Schreiber, S. L. (1990). Two distinct signal transmission pathways in lymphocytes-T cells are inhibited by complexes formed between an immunophilin and either FK506 or rapamycin. *Proc. Natl Acad. Sci. USA*, **87**, 9231-9235.
- Brandts, J. F., Halvorson, H. R. & Brennan, M. (1975). Consideration of the possibility that the slow step in protein denaturation reactions is due to *cis-trans* isomerism of proline residues. *Biochemistry*, **14**, 4953-4963.
- Burton, R. E., Huang, G. S., Daugherty, M. A., Fullbright, P. W. & Oas, T. G. (1996). Microsecond protein folding through a compact transition state. *J. Mol. Biol.* **263**, 311-322.
- CammersGoodwin, A., Allen, T. J., Oslick, S. L., McClure, K. F., Lee, J. H. & Kemp, D. S. (1996). Mechanism of stabilization of helical conformations

- of polypeptides by water containing trifluoroethanol. *J. Am. Chem. Soc.* **118**, 3082-3090.
- Chan, C. K., Hu, Y., Takahashi, S., Rousseau, D. L., Eaton, W. A. & Hofrichter, J. (1997). Submillisecond protein folding kinetics studied by ultrarapid mixing. *Proc. Natl Acad. Sci. USA*, **94**, 1779-1784.
- Chen, B., Baase, W. A. & Schellman, J. A. (1989). Low temperature unfolding of a mutant of phage T4 lysozyme. 2. Kinetic investigations. *Biochemistry*, **26**, 691-699.
- Chiti, F., Taddei, N., Van Nuland, N. A. J., Magherini, F., Stefani, M., Ramponi, G. & Dobson, C. M. (1998). Structural characterisation of the transition state for folding of muscle acylphosphatase. *J. Mol. Biol.* **283**, 893-903.
- Chiti, F., Taddei, N., Webster, P., Hamada, D., Fiaschi, T., Ramponi, G. & Dobson, C. M. (1999). Acceleration of the folding of acylphosphatase by stabilisation of local secondary structure. *Nature Struct. Biol.* **6**, 380-387.
- Daggett, V., Li, A. J., Itzhaki, L. S., Otzen, D. E. & Fersht, A. R. (1996). Structure of the transition-state for folding of a protein-derived from experiment and simulation. *J. Mol. Biol.* **257**, 430-440.
- Daggett, V., Li, A. & Fersht, A. R. (1998). A combined molecular dynamics and  $\phi$ -value analysis of structure-reactivity relationships in the transition state and unfolding pathway of barnase: the structural basis of Hammond and anti-Hammond effects. *J. Am. Chem. Soc.* **120**, 12740-12754.
- Egan, D. A., Logan, T. M., Liang, H., Matayoshi, E., Fesik, S. W. & Holzman, T. F. (1993). Equilibrium denaturation of recombinant human FK506 binding protein in urea. *Biochemistry*, **32**, 1920-1927.
- Evans, P. A. & Radford, S. E. (1994). Probing the structure of folding intermediates. *Curr. Opin. Struct. Biol.* **4**, 100-106.
- Fersht, A. R. (1995). Optimization of rates of protein folding: the nucleation-collapse mechanism for the folding of chymotrypsin inhibitor 2 (CI2) and its consequences. *Proc. Natl Acad. Sci. USA*, **92**, 10869-10873.
- Fersht, A. R., Matouschek, A. & Serrano, L. (1992). The folding of an enzyme. 1. Theory of protein engineering analysis of stability and pathway of protein folding. *J. Mol. Biol.* **224**, 771-782.
- Fulton, K. F., Main, E. R. G., Daggett, V. & Jackson, S. E. (1999). Mapping the interactions present in the transition state for folding/unfolding of FKBP12. *J. Mol. Biol.* **???**, ???-???
- Grathwohl, C. & Wuthrich, K. (1981). NMR-studies of the rates of proline *cis-trans* isomerization in oligopeptides. *Biopolymers*, **20**, 2623-2633.
- Jackson, S. E. (1998). How do small single-domain proteins fold?. *Fold. Design*, **3**, R81-R90.
- Jackson, S. E. & Fersht, A. R. (1991a). Folding of chymotrypsin inhibitor-2. 1. Evidence for a two-state transition. *Biochemistry*, **30**, 10428-10435.
- Jackson, S. E. & Fersht, A. R. (1991b). Folding of chymotrypsin inhibitor-2. 2. Influence of proline isomerization on the folding kinetics and thermodynamic characterization of the transition state of folding. *Biochemistry*, **30**, 10436-10443.
- Jackson, S. E., Moracci, M., El Masry, N., Johnson, C. M. & Fersht, A. R. (1993). Effect of cavity-creating mutations in the hydrophobic core of chymotrypsin inhibitor-2. *Biochemistry*, **32**, 11259-11269.
- Kay, J. E. (1996). Structure-function relationships in the FK506-binding protein (FKBP) family of peptidyl prolyl isomerases. *Biochem. J.* **314**, 361-385.
- Khorasanizadeh, S., Peters, I. D. & Roder, H. (1996). Evidence for a three-state model of protein folding from kinetic analysis of ubiquitin variants with altered core residues. *Nature Struct. Biol.* **3**, 193-205.
- Kim, P. S. & Baldwin, R. L. (1982). Specific intermediates in the folding reactions of small proteins and the mechanism of protein folding. *Annu. Rev. Biochem.* **51**, 459-489.
- Kraulis, P. (1991). MOLSCRIPT: a program to produce both detailed and schematic plots of protein structures. *J. Appl. Crystallog.* **24**, 946-950.
- Ladurner, A. G., Itzhaki, L. S., Daggett, V. & Fersht, A. R. (1998). Synergy between simulation and experiment in describing the energy landscape of protein folding. *Proc. Natl Acad. Sci. USA*, **95**, 8473-8478.
- Levinthal, C. (1968). Are there pathways for protein folding?. *J. Chim. Phys.* **85**, 44-45.
- Li, A. J. & Daggett, V. (1996). Identification and characterization of the unfolding transition-state of chymotrypsin inhibitor 2 by molecular-dynamics simulations. *J. Mol. Biol.* **257**, 412-429.
- Logan, T., Theriault, Y. & Fesik, S. (1994). Structural characterization of the FK506 binding-protein unfolded in urea and guanidine-hydrochloride. *J. Mol. Biol.* **236**, 637-648.
- Lu, H., Buck, M., Radford, S. E. & Dobson, C. M. (1997). Acceleration of the folding of hen lysozyme by trifluoroethanol. *J. Mol. Biol.* **265**, 112-117.
- Main, E. R. G., Fulton, K. F. G. & Jackson, S. E. (1998). "Stability of FKBP12: The Context-dependent Nature of Destabilising Mutations". *Biochemistry* **37**, 6145-6153.
- Main, E. R. G. & Jackson, S. E. (1999). Does trifluoroethanol affect folding pathways and can it be used as a probe of structure in transition states? *Nature Struct. Biol.* **in the press**.
- Matouschek, A. & Fersht, A. R. (1993). Application of physical organic chemistry to engineered mutants of proteins-Hammond Postulate behavior in the transition state of protein folding. *Proc. Natl Acad. Sci. USA*, **90**, 7814-7818.
- Matouschek, A. T. E. L., Otzen, D. E., Itzhaki, L. S., Jackson, S. E. & Fersht, A. R. (1995). Movement of the position of the transition state in protein folding. *Biochemistry*, **34**, 13656-13662.
- Meiering, E. M. (1992). Studies on the active site of barnase. PhD thesis, Cambridge University.
- Merritt, E. A. & Murphy, M. E. P. (1994). Raster3D version 2.0-a program for photorealistic molecular graphics. *Acta Crystallog. Sect. D*, **50**, 869-873.
- Michnick, S. W., Rosen, M. K., Wandless, T. J., Karplus, M. & Schreiber, S. L. (1991). Aolution structure of FKBP, a rotamase enzyme and receptor for FK506 and rapamycin. *Science*, **252**, 836-842.
- Mines, G. A., Pascher, T., Lee, S. C., Winkler, J. R. & Gray, H. B. (1996). Cytochrome-c folding triggered by electron-transfer. *Chem. Biol.* **3**, 491-497.
- Narhi, L. O., Philo, J. S., Li, T. S., Zhang, M., Samal, B. & Arakawa, T. (1996). Induction of  $\alpha$ -helix in the  $\beta$ -sheet protein tumor necrosis factor- $\alpha$ : Acid-induced denaturation. *Biochemistry*, **35**, 11454-11460.
- Nelson, J. W. & Kallenbach, N. R. (1989). Persistence of the  $\alpha$ -helix stop signal in the S-peptide in TFE Solutions. *Biochemistry*, **28**, 5256-5261.

- Plaxco, K. W., Simons, K. T. & Baker, D. (1998). Contact order, transition state placement and the refolding rates of single domain proteins. *J. Mol. Biol.* **277**, 985-994.
- Robertson, A. D. & Murphy, K. P. (1997). Protein structure and the energetics of protein stability. *Chem. Rev.* **97**, 1251-1267.
- Sancho, J., Meiering, E. & Fersht, A. R. (1991). Mapping transition states of protein unfolding by protein engineering of ligand-binding sites. *J. Mol. Biol.* **221**, 1007-1014.
- Schindler, T., Herrler, M., Marahiel, M. A. & Schmid, F. X. (1995). Extremely rapid folding in the absence of intermediates. *Nature Struct. Biol.* **2**, 663-673.
- Schmid, F. X., Frech, C., Scholz, C. & Walter, S. (1996). Catalyzed and assisted protein folding of ribonuclease T1. *Biol. Chem.* **377**, 417-424.
- Scholz, C., Zarnt, T., Kern, G., Lang, K., Burtscher, H., Fischer, G. & Schmid, F. X. (1996). Autocatalytic folding of the folding catalyst FKBP12. *J. Biol. Chem.* **271**, 12703-12707.
- Schreiber, G. & Fersht, A. R. (1993). The refolding of *cis*-peptidylprolyl and *trans*-peptidylprolyl isomers of barstar. *Biochemistry*, **32**, 11195-11203.
- Sivaraman, T., Kumar, T. K. S. & Yu, C. (1996). Destabilisation of native tertiary structural interactions is linked to helix-induction by 2,2,2-trifluoroethanol in proteins. *Int. J. Biol. Macromol.* **19**, 235-239.
- Tanford, C. (1968). Protein denaturation. *Advan. Protein Chem.* **23**, 121-282.
- Tanford, C. (1970). Protein folding. Part C. *Advan. Protein Chem.* **24**, 1-95.
- van Duyne, G. D., Standaert, R. F., Karplus, P. A., Schreiber, S. L. & Clardy, J. (1991). Atomic-structure of FKBP-FK506, an immunophilin-immunosuppressant complex. *Science*, **252**, 839-842.
- van Nuland, N. A. J., Meijberg, W., Warner, J., Forge, V., Scheek, R. M., Robillard, G. T. & Dobson, C. M. (1998). Slow cooperative folding of a small globular protein HPr. *Biochemistry*, **37**, 622-637.
- Veeraghavan, S., Holzman, T. F. & Nall, B. (1996). Autocatalyzed protein folding. *Biochemistry*, **35**, 10601-10607.
- Walgers, R., Lee, T. C. & CammersGoodwin, A. (1998). An indirect chaotropic mechanism for the stabilization of helix conformation of peptides in aqueous trifluoroethanol and hexafluoro-2-propanol. *J. Am. Chem. Soc.* **120**, 5073-5079.

*Edited by J. Thornton*

*(Received 26 November 1998; received in revised form 24 May 1999; accepted 10 June 1999)*